

Supplementary information for

Interaction of NBD-labelled fatty amines with liquid-ordered membranes: a combined molecular dynamics simulation and fluorescence spectroscopy study

Hugo A. L. Filipe^{1,2,3}, David Bowman^{2,3}, Tiago Palmeira^{1,2}, Renato M. S. Cardoso^{1,2}, Luís M. S. Loura^{1,3,4*}, Maria João Moreno^{1,2,3*}

1 – Centro de Química de Coimbra, Largo D. Dinis, Rua Larga, 3004-535 Coimbra, Portugal

2 - Departamento de Química, Faculdade de Ciências e Tecnologia, Universidade de Coimbra, Largo D. Dinis, Rua Larga, 3004-535 Coimbra, Portugal

3 - Centro de Neurociências e Biologia Celular, Universidade de Coimbra, 3004-504 Coimbra, Portugal

4 – Faculdade de Farmácia, Universidade de Coimbra, Pólo das Ciências da Saúde, Azinhaga de Santa Comba, 3000-548 Coimbra, Portugal

* Corresponding authors

Telephone: +351 239854481; Fax: +351 239827703; E-mail: mmoreno@ci.uc.pt

Telephone: +351 239488485; Fax: +351 239827126; E-mail: lloura@ff.uc.pt

RESULTS FROM MOLECULAR DYNAMICS SIMULATIONS

Location of the NBD fluorophore with different force fields. Figure S1 shows the comparison between the transverse position $\langle z \rangle$ of the NBD group and the membrane lipids with different force fields. The area per lipid of the POPC with the GROMOS53A6 parameterisation is $a = 0.641 \pm 0.020 \text{ nm}^2$, similar to $a = 0.625 \pm 0.015 \text{ nm}^2$ obtained in our previous paper¹ with the GROMOS87 force field modified by Berger et al.². The order parameter profiles obtained using both parameterisations are shown in Figure S2. The results obtained are similar, with slightly lower values for the GROMOS53A6 force field, in accordance with the higher area per lipid obtained with this parameterisation.

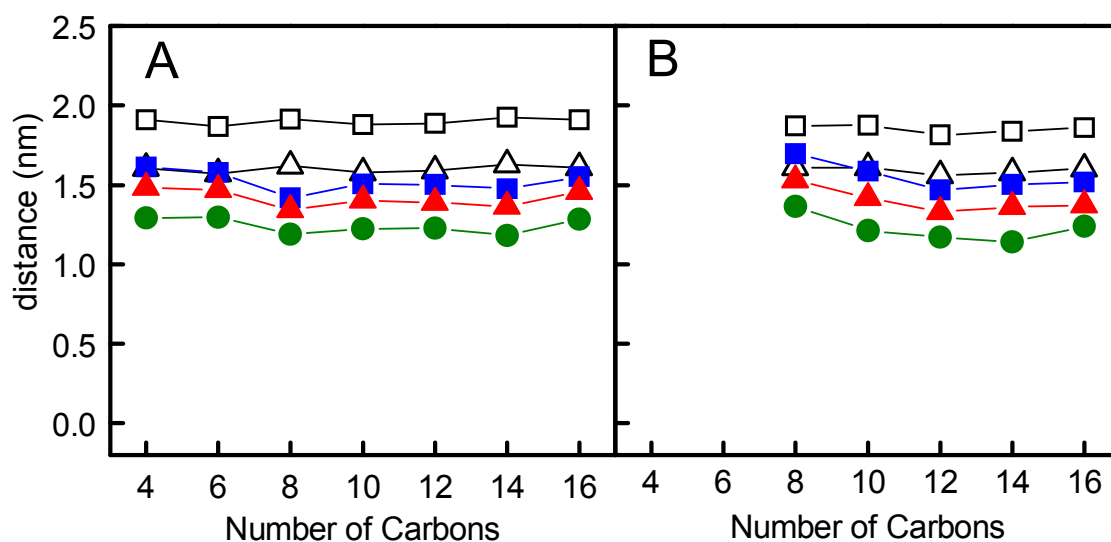


Figure S1 – Comparison between the average transverse positions $\langle z \rangle$ of some relevant atoms of POPC and the amphiphiles NBD group, for NBD-C_n with distinct number of carbons in the alkyl chain (n), simulated with different force fields: (A), GROMOS87 and (B) GROMOS53A6. The host lipid atoms represented are P8 (open squares) and C13 (open triangles). The amphiphiles are represented by N1 (olive), N6 (blue) and NBD COM (red).

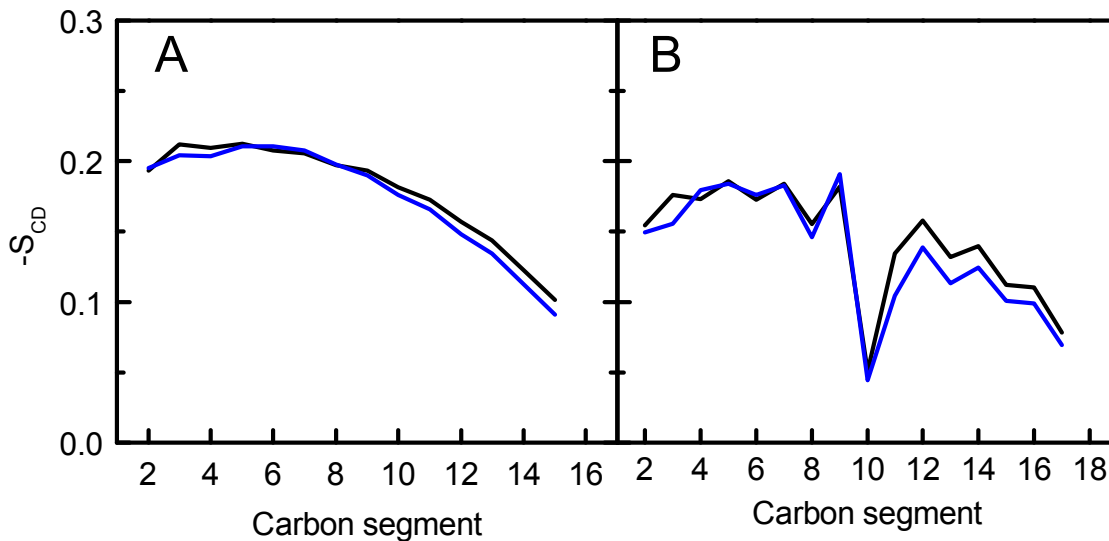


Figure S2 – Deuterium order parameter of the POPC *sn*-1 (A) and *sn*-2 (B) chains simulated using different force fields: GROMOS87 (black) and GROMOS53A6 (blue).

Equilibration of the cholesterol containing systems. The equilibration of the cholesterol containing bilayers was assessed by the time evolution of the area per lipid and by the location of the fluorophore in each simulation. As shown in Figure S3, the POPC/Chol (1:1) bilayers were already equilibrated at the beginning of the simulations, whereas the SpM/Chol (6:4) bilayer rapidly approached equilibrium. Complete equilibration of the bilayers, including the NBD location, shown in Figure S4, was achieved in less than 20 ns, validating the use of the last 80 ns of the full length simulations for analysis.

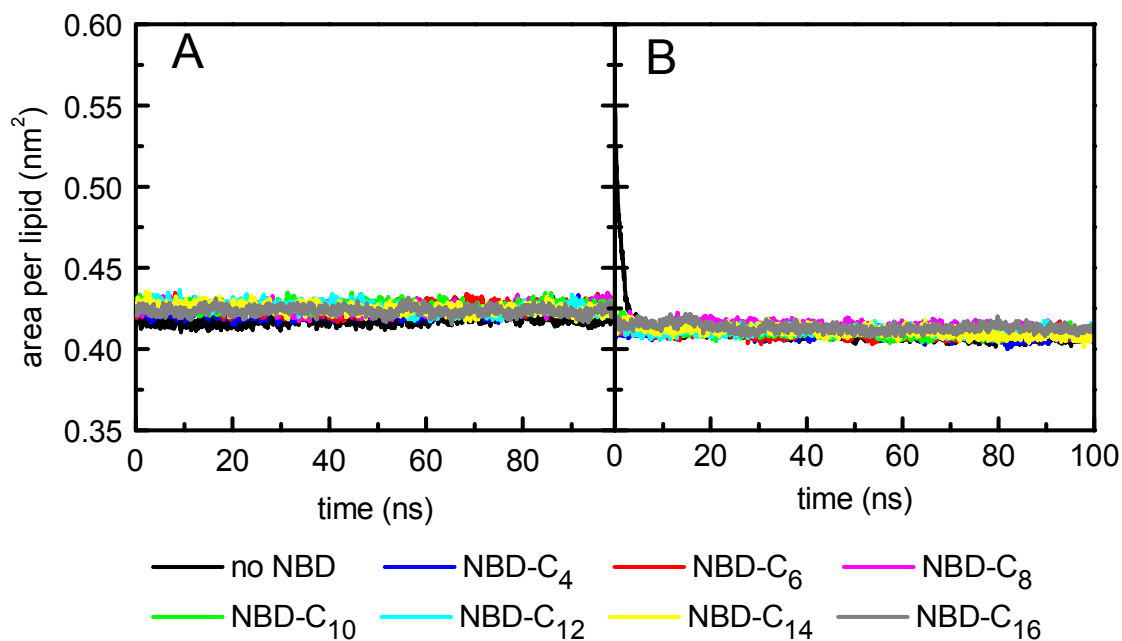


Figure S3 – Time variation of the area per lipid for (A) POPC/Chol and POPC/Chol/NBD-C_n systems, and (B) SpM/Chol and SpM/Chol/NBD-C_n systems, for lipid bilayers without and with the NBD-C_n amphiphiles as indicated in the figure.

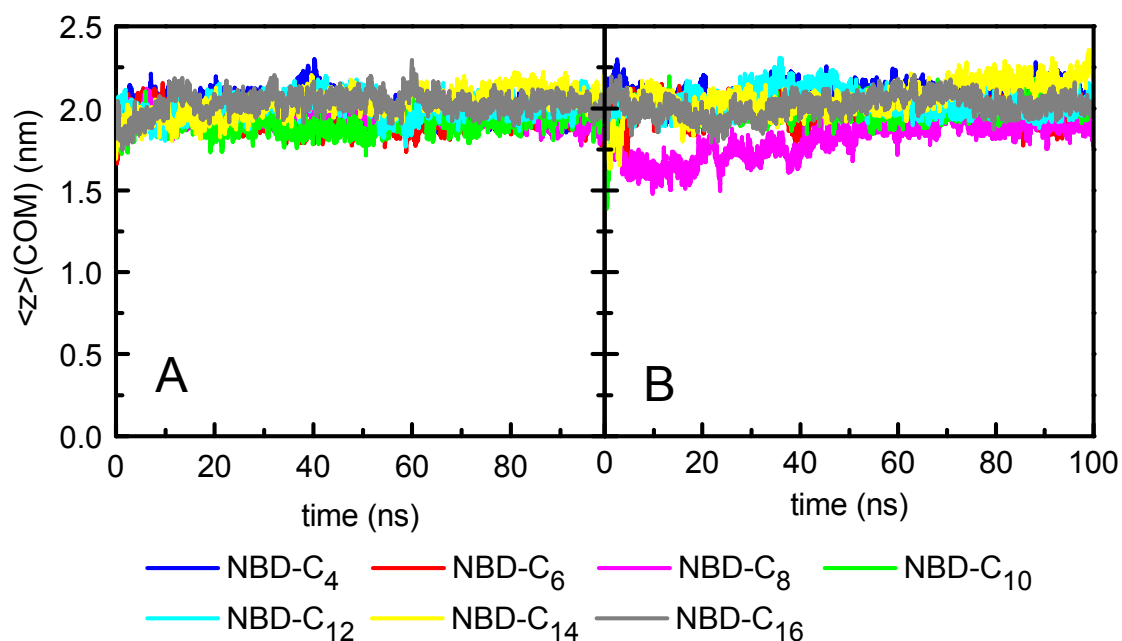


Figure S4 – Time variation of the $\langle z \rangle(\text{COM})$ distance of the NBD group to the center of the bilayer for: (A) POPC/Chol/NBD systems, and for (B) SpM/Chol/NBD systems, for lipid bilayers without and with the NBD-C_n amphiphiles as indicated in the figure..

Deuterium order parameters. The order parameter profiles, $-S_{CD}$, calculated for both chains of POPC and SpM are shown in Figure S5. The profiles obtained agree well with both experimental and simulated data for POPC/Chol,³⁻⁵ as well as for SpM/Chol^{3, 6, 7} bilayers. Incorporation of NBD- C_n does not induce any significant perturbation in the bilayer.

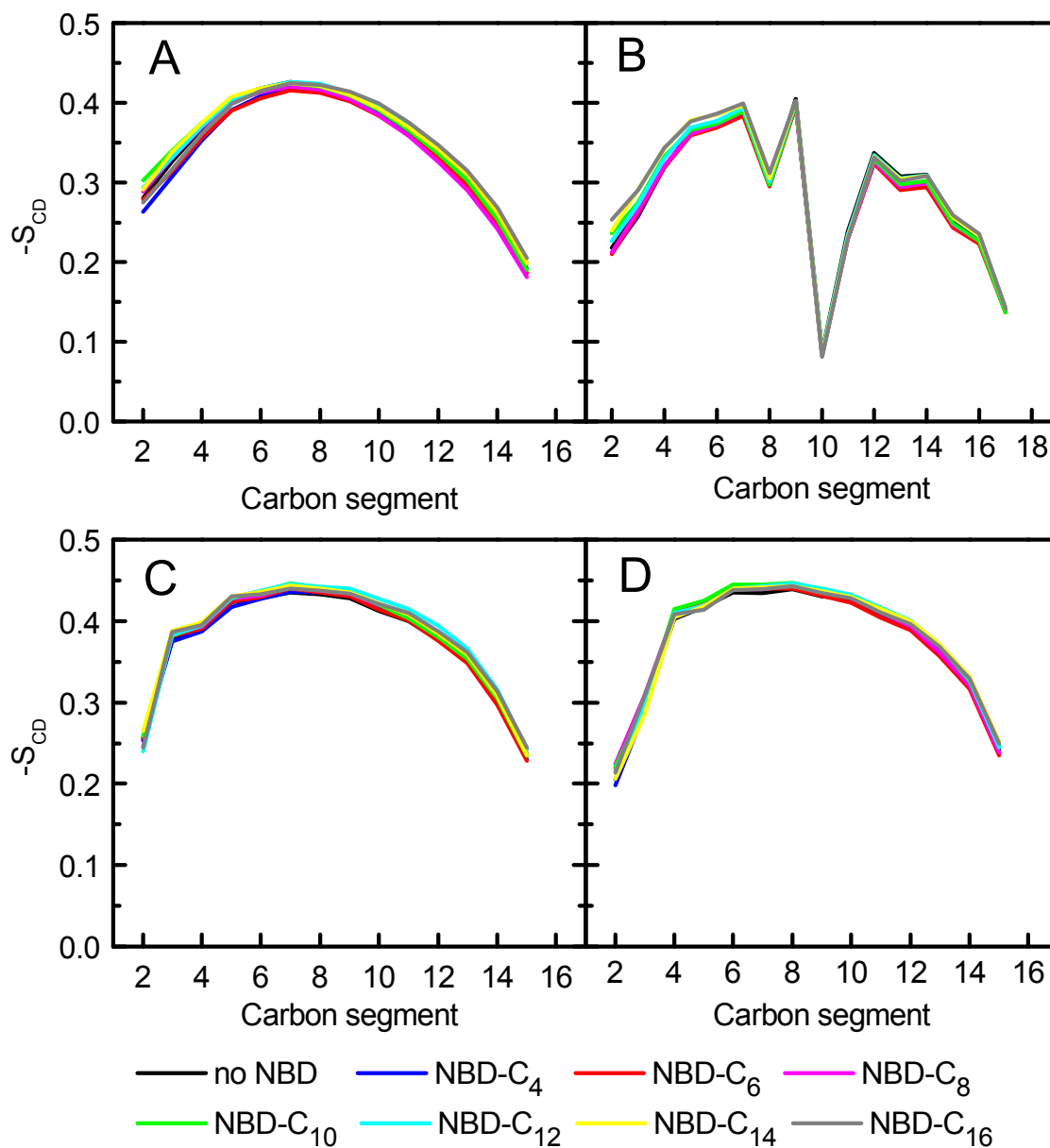


Figure S5 – Deuterium order parameter of the POPC *sn*-1 (A) and *sn*-2 (B), and SpM acyl (C) and sphingosine (D) chains, for lipid bilayers without and with the NBD- C_n amphiphiles as indicated in the figure.

Lateral Diffusion. Lateral diffusion coefficients D were calculated from the two-dimensional mean squared displacement (MSD), using the Einstein relation

$$D = \frac{1}{4} \lim_{t \rightarrow \infty} \frac{d\text{MSD}(t)}{dt} \quad (1)$$

In turn, MSD is defined by

$$\text{MSD}(t) = \left\langle \left\| \vec{r}_i(t+t_0) - \vec{r}_i(t_0) \right\|^2 \right\rangle \quad (2)$$

where \vec{r}_i is the (x, y) position of the centre of mass of molecule i of a given species, and the averaging is carried out over all molecules of this kind from the initial time considered t_0 . To eliminate noise due to fluctuations in the centre of mass of each monolayer, all MSD analyses were carried out using trajectories with fixed centre of mass of one of the monolayers, and the final result is averaged over the two leaflets.

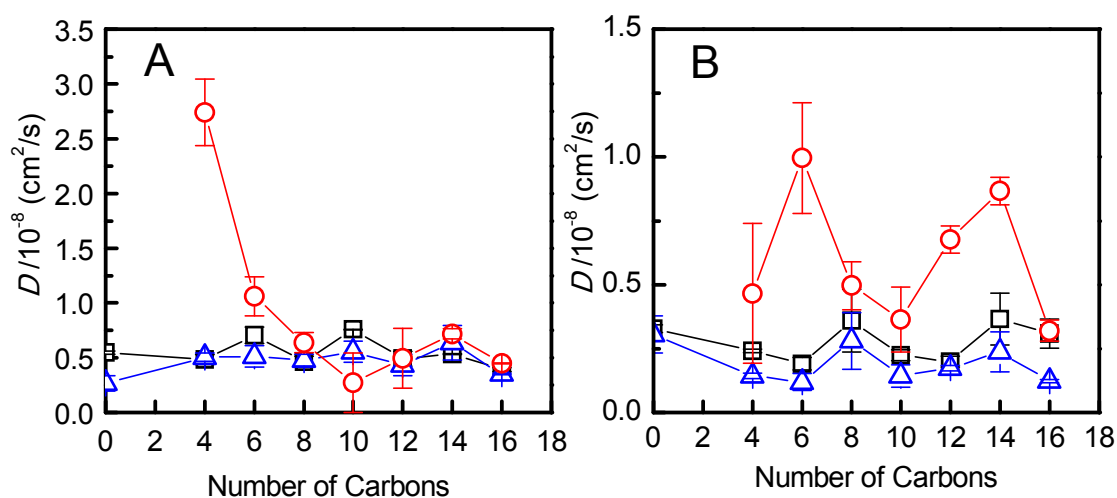


Figure S6 – Diffusion coefficients of (A) POPC (black), Chol (blue) and NBD- C_n (red) in POPC/Chol/NBD- C_n and (B) SpM (black), Chol (blue) and NBD- C_n (red) in SpM/Chol/NBD- C_n bilayers. The x axis is the length of the NBD- C_n alkyl chain incorporated in the lipid bilayer, with 0 representing the bilayer without NBD- C_n .

Electrostatic Potential. The electrostatic potential across the bilayer (z coordinate) was calculated by double integration of the charge density:

$$\Delta\psi(z) = \psi(z) - \psi(\infty) = -\frac{1}{\epsilon_0} \int_z^\infty dz' \int_{z'}^\infty \rho(z'') dz'' \quad (3)$$

In this calculation, the positions of all atoms were determined relative to the instantaneous centre of mass ($z = 0$) in all simulations, for each frame. The potential was also averaged and symmetrised for the two bilayer leaflets.⁸

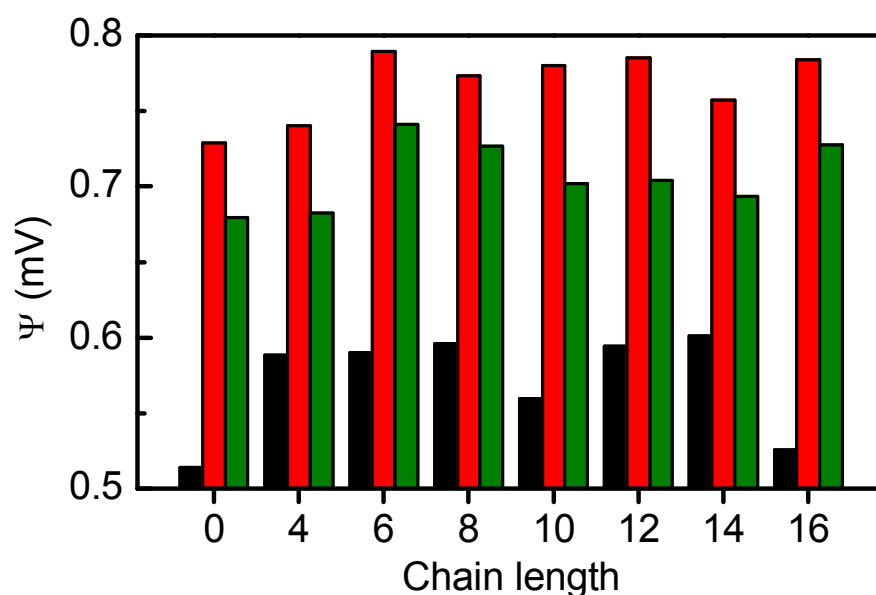


Figure S7 – Electrostatic potential in the center of the bilayer (relative to the water region) as a function of the total number of carbons of the NBD- C_n alkyl chains in POPC¹ (black), POPC/Chol (red) and SpM/Chol (olive) bilayers. An abscissa equal to zero corresponds to the absence of amphiphile.

PHOTOPHYSICAL CHARACTERISATION OF NBD-C_n IN POPC/CHOL BILAYERS

Fluorescence quantum yields. The fluorescence emission spectra of NBD-C_n in POPC/Chol (1:1) bilayers are shown in Figure S8, together with that of NBD-DMPE in POPC membranes, which was used as a reference. The lipid bilayers were prepared with a NBD-C_n to lipid ratio of 1:400. However, for $n \leq 10$ a significant amount of NBD-C_n was retained in the polycarbonate filters during the extrusion steps in the preparation of the liposomes, leading to a smaller concentration in the final preparation. This reflects the low affinity of the amphiphiles with small alkyl chains for cholesterol enriched membranes. The fluorescence emission spectra shown in Figure S8 have been normalised for the intensity of light absorbed by each NBD-C_n derivative. The normalised emission spectra are displayed in the inset, showing small (non-significant) deviations in the emission maxima except for NBD-C₈, which is shifted towards lower energies (larger wavelengths) in agreement with a poor anchoring in the POPC/Chol bilayer.

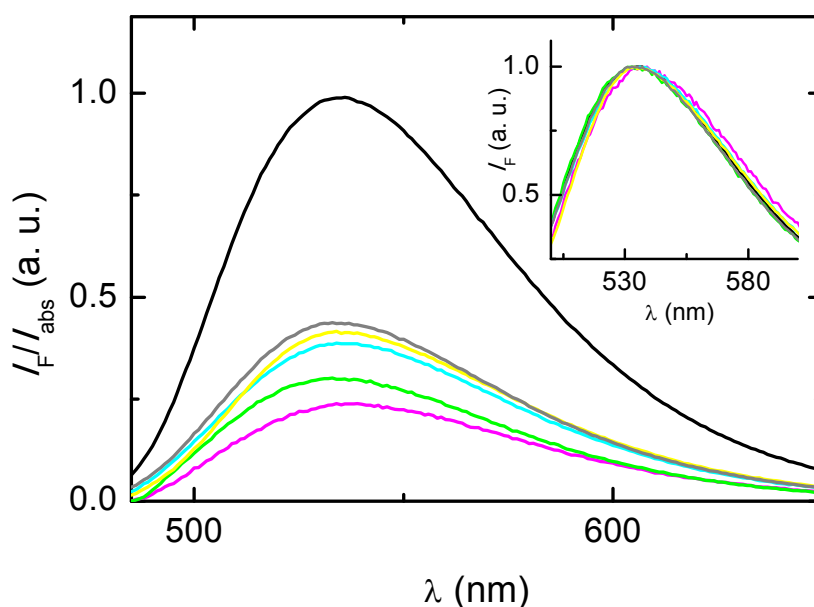


Figure S8 – Fluorescence emission spectra of NBD-C_n inserted in POPC/Chol (1:1) bilayers, NBD-C₈ (—), NBD-C₁₀ (—), NBD-C₁₂ (—), NBD-C₁₄ (—) and NBD-C₁₆ (—), and NBD-DMPE (—) in POPC bilayers. The inset shows the fluorescence emission spectra normalised at the maximum intensity. The excitation wavelength was 460 nm and the temperature was 25 °C.

Fluorescence lifetimes. As observed for NBD- C_n in POPC bilayers,⁹ the fluorescence decay in POPC/Chol (1:1) bilayers was complex, being well described by a bi-exponential function. The lifetime and amplitude of the two components are given in Figure S9, together with the results obtained in POPC,⁹ and the average lifetime (weighted by the fluorescence intensity) is given in the manuscript (Figure 11B). The lifetime of the short component is essentially the same for all amphiphiles in both bilayers (ca. 2 ns) while the long component decreases as the length of the alkyl chain increases. The amplitude of both components is essentially independent on the length of the alkyl chain for both bilayers, but the weight of the long component is significantly smaller in the ordered POPC/Chol bilayer. The decrease in the contribution of the long component, together with the small decrease in the respective lifetime, leads to a smaller average lifetime of NBD- C_n in POPC/Chol (1:1) bilayers (Figure 11 in the manuscript).

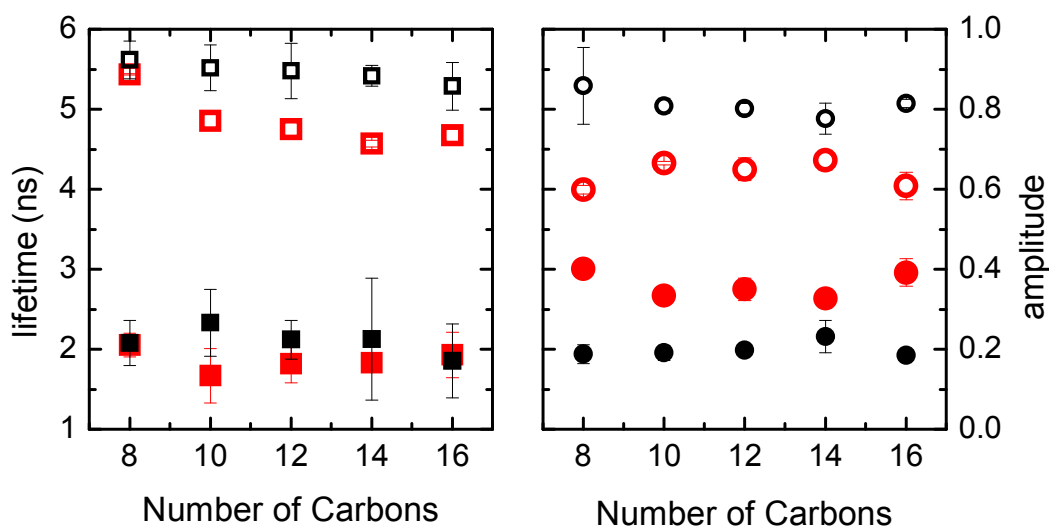


Figure S9 – Fluorescence lifetimes (left) and respective amplitudes (right) of NBD- C_n in POPC¹ (black) and in POPC/Chol (red). The solid symbols correspond to the longer lifetime component and respective amplitude, while the open symbols correspond to the short lived component.

Ionisation constants. In the alkaline region of pH, the NBD group changes its ionisation state and becomes non-fluorescent. The effect of the aqueous media pH value in the fluorescence intensity at 530 nm is shown in Figure S10 (plot A) for the case of NBD- C_{10}

inserted in POPC/Chol (1:1) bilayers, the emission spectra being given in the inset. The data are well described by a single ionisation equilibrium in this pH range, with the negatively charged form being non-fluorescent. The results obtained for the remaining amphiphiles in the NBD- C_n homologous series are shown in plot B, and the apparent pK_a values are shown in the manuscript (Figure 11C).

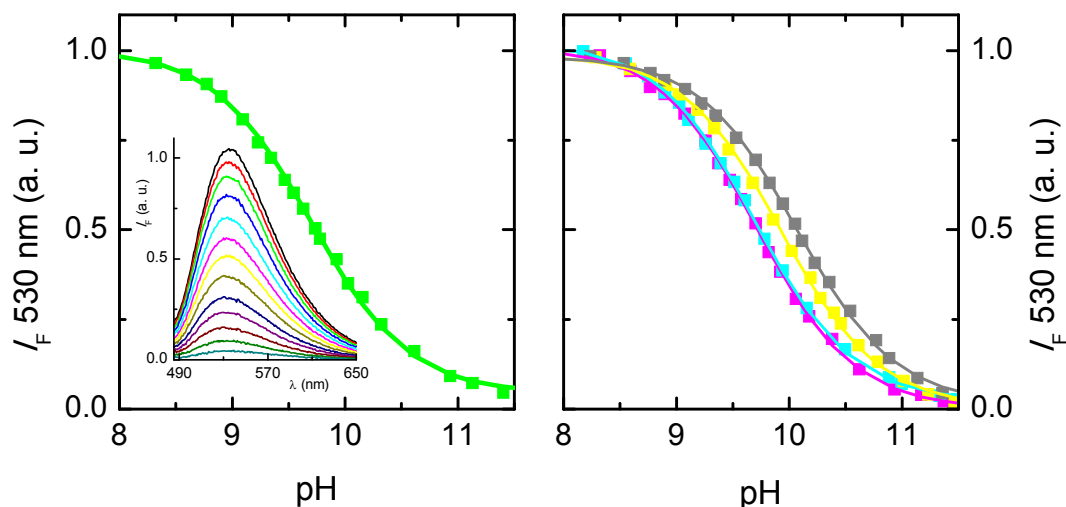


Figure S10 – Effect of the pH value in the bulk aqueous phase in the fluorescence emission intensity at 530 nm, when excited at 475 nm, for NBD- C_n inserted in POPC/Chol (1:1) at 25 °C. Results obtained for NBD- C_{10} (left), the inset shows the fluorescence emission spectra, as well as for NBD- C_8 (■), NBD- C_{12} (■), NBD- C_{14} (■) and NBD- C_{16} (■) (right). The lines are the best fit with a single ionisation equilibrium.

Steady-state fluorescence anisotropy. The fluorescence anisotropy of NBD- C_n inserted in POPC/Chol (1:1) bilayers is shown in Figure S11. No significant dependence on the emission wavelength was observed in the range 540-560 nm, except for NBD- C_8 that shows a small decrease for longer wavelengths. The average value of the anisotropy is shown in Figure 11D of the manuscript. A small increase in the steady state fluorescence anisotropy with the length of the alkyl chain in NBD- C_n is observed, reflecting the decrease in the average fluorescence lifetime along the homologous series.

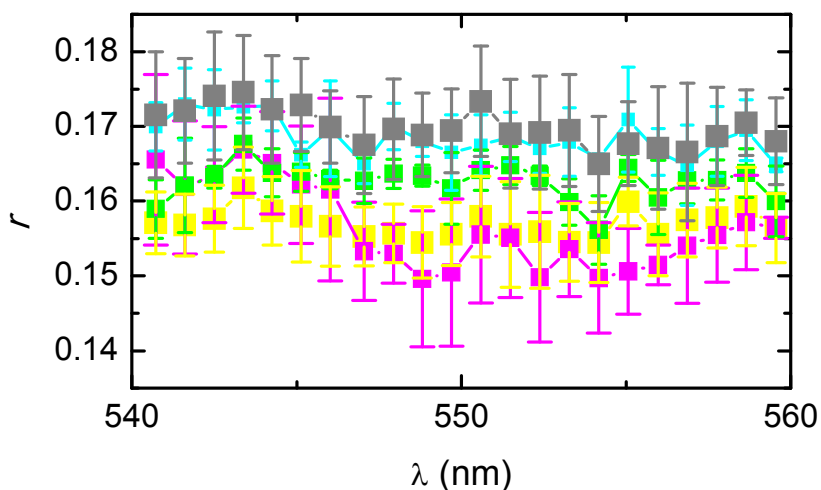


Figure S11 – Steady-state fluorescence anisotropy of NBD-Cn inserted in POPC/Chol (1:1) bilayers ($\lambda_{exc}=475$ nm), for NBD-C₈ (■), NBD-C₁₀ (■), NBD-C₁₂ (■), NBD-C₁₄ (■) and NBD-C₁₆ (■).

References

1. H. A. L. Filipe, M. J. Moreno and L. M. S. Loura, *J. Phys. Chem. B*, 2011, **115**, 10109-10119.
2. O. Berger, O. Edholm and F. Jahnig, *Biophys. J.*, 1997, **72**, 2002-2013.
3. Z. Zhang, S. Y. Bhide and M. L. Berkowitz, *J. Phys. Chem. B*, 2007, **111**, 12888-12897.
4. T. M. Ferreira, F. Coreta-Gomes, O. H. S. Ollila, M. J. Moreno, W. L. C. Vaz and D. Topgaard, *Phys. Chem. Chem. Phys.*, 2013, **15**, 1976-1989.
5. A. M. T. Martins do Canto, A. J. Palace Carvalho, J. P. Prates Ramalho and L. M. S. Loura, *J. Mol. Struct.: THEOCHEM*, 2010, **946**, 119-124.
6. J. Zidar, F. Merzel, M. Hodošček, K. Rebolj, K. Sepčić, P. Maček and D. a. Janežič, *J. Phys. Chem. B*, 2009, **113**, 15795-15802.
7. A. M. T. M. do Canto, P. D. Santos, J. Martins and L. M. S. Loura, *Colloids Surf., A*, 2015, **480**, 296-306.
8. D. P. Tieleman and H. J. C. Berendsen, *J. Chem. Phys.*, 1996, **105**, 4871-4880.
9. R. M. S. Cardoso, H. A. L. Filipe, F. Gomes, N. D. Moreira, W. L. C. Vaz and M. J. Moreno, *J. Phys. Chem. B*, 2010, **114**, 16337-16346.